***Winery wastes as precursors of sustainable porous carbons for environmental applications**

Laura Guardia, Loreto Suárez, Nausika Querejeta, Covadonga Pevida,

Teresa A. Centeno[1]

Instituto Nacional del Carbón (INCAR-CSIC). Francisco Pintado Fe, 26. 33011 Oviedo (Spain)

Abstract

An efficient alternative for the management and valorization of the huge amount of seasonal wastes generated by winery industries is shown. Sustainable porous carbons were successfully prepared by one-pot activation of grape bagasse, stalks and oil free-seeds. Benefiting from the high moisture of these residues, a prior hydrothermal carbonization increases the activation yield and generates carbons with less oxygen content and inorganic impurities. The mild physical or chemical activation of winery wastes resulted in highly microporous carbons with specific surface S_{BET} up to 2053 m^2/g and great potential for environmental protection and electrical energy storage. They are excellent sorbents for CO_2 capture under post- and pre-combustion conditions (16 and 69 wt%, respectively) and achieve superior electrochemical capacitance of nearly 300 F/g in aqueous electrolyte and 180 F/g in ionic liquid based-medium.

Keywords: Winery waste, activated carbon, hydrothermal carbonization, CO_2 capture, supercapacitor

[1] Corresponding author
E-mail address: teresa@incar.csic.es (T.A. Centeno)

1. Introduction

According to the recent report of the International Organization of Vine and Wine (OIV), wine production remains one of the most important agricultural activities in the world. In 2016, the area under vines rose to 7.5 mha worldwide and the production (excluding juice and musts) reached 267 mhl (Aurand, 2015).

Winery activities generate huge amounts of seasonal wastes and their management is already becoming an acute problem of storage and elimination in both ecological and economic terms. It has been estimated that from 100 kg of grapes derive around 25 kg of residues, about 70% are grape skins, 12% of stalks and 18% of seeds (Toscano et al., 2013). Their high humidity and nutrients content provoke bacteria growth and uncontrolled emission of greenhouse gases. Landfilling is a great risk of spreading pests and diseases and the seeping down of alcohol and organic acids must also be prevented in order to avoid negative effects on soil and groundwater.

The traditional approach to revalue the grape marc by distillation has been much reduced due to the steady decline in the spirit beverages market in recent years. Moreover, this process also produces exhausted grape marc and harmful vinasse which require subsequent disposal (Zhang et al., 2017). Grape pomace may be also recovered in the form of animal feed but it needs a previous drying for storage. With regard to stalks and other residues with low economic value, landfilling in large dumps and incineration are the most commonly used processes for management.

In this context, winery industry is urging recycling alternatives to profit the wastes through their use as raw of added-value materials (Muhlack et al., 2017). Thus, a variety of technologies have been proposed to extract a great range of functional components such as natural antioxidants, biosurfactants, bioemulsifiers, ethanol, tartrates, citric acid,

anthocyanins, polyphenols, dietary fiber, etc. from grape pomace (Arvanitoyannis et al., 2008; Devesa-Rey et al., 2011; Dwyer et al., 2014; Muhlack et al., 2017). Seeds separation from grape marc and subsequent extraction allows to obtain an oil highly appreciated in food and cosmetics markets (Dwyer et al., 2014; Toscano et al., 2013). Grape seed extracts with antioxidant activity also show potential as nutritional supplement for humans and animals (González-Paramás et al., 2004; O'Grady et al., 2008). However, these approaches still have to prove their profitable viability on a large scale (Dwyer et al., 2014) and, as far as they recover only part of the components, share many of the disposal concerns of the raw wastes.

Much attention is also being paid to winery wastes for their richness in compounds of great interest for soil fertility (Arvanitoyannis et al., 2008; Muhlack et al., 2017) although the presence of certain polyphenols with phytotoxic and antimicrobial effects may hinder their direct use (Bustamante et al., 2008). In recent years composting and anaerobic digestion are being implemented to obtain soil conditioners and high-grade organic fertilizers (Arvanitoyannis et al., 2008; Devesa-Rey et al., 2011; Muhlack et al., 2017; Zhang et al., 2017) and biogas (El Achkar et al., 2016).

The growing interest in obtaining energy from biomass has stimulated studies on the possibilities for the disposal of winery wastes by thermal decomposition. Combustion is an effective mean to reduce the total amount of residues (Muhlack et al., 2017; Zhang et al., 2017). It has been estimated that the potential energy content of the residual biomass from a hectare of grapevine is around 19 GJ of gross energy although the high content of water and ashes of these by-products critically reduce the combustion efficiency (Toscano et al., 2013).

The detailed analysis by Zhang et al. (2017) revealed that pyrolysis is more economically viable than combustion and exhibits a great minimisation of residues by producing 151 kg of biochar and 140 kg of biofuel per tonne of grape marc.

The humidity of the winery wastes is a disadvantage to their transport and clearly detrimental to the energetic efficiency of their thermochemical processing. Therefore, alternatives compatible with the presence of water such as hydrothermal carbonization (HTC) result really interesting. The strength of this technology relies precisely in the transformation of wet feedstocks without the drying pre-treatment of traditional approaches. Requiring milder operation conditions (generally 180-250°C and 20-40 bar) with respect to the other treatments (Kambo and Dutta, 2015), HTC presents a more affordable technical applicability. The products are primarily a solid phase enriched in carbon (hydrochar), a liquid phase with dissolved organic compounds and a small quantity of gases (Kambo and Dutta, 2015). Pala et al. (2014) have found higher energy densification and energy yield by HTC of grape pomace than by torrefaction whereas the aqueous phase displayed antioxidant activity. More recent studies support hydrothermal treatment of grape marc as an efficient pathway for producing CO_2 neutral solid fuels on-site at the wineries (Lucian and Fiori, 2017; Mäkelä et al., 2017). Along with obtaining fuels, several high-valuable chemicals were also found in the aqueous phase. Yedro et al. (2015) reported the successful extraction of polyphenols and the production of oil, pentose and hexose sugars as well as lignin from grape seeds by HTC.

The current expansion of applications of porous carbons (Titirici et al., 2015) has encouraged research on low-cost sustainable materials. The elimination of winery wastes and above all the production of carbons with the highest performance from them would imply a significant advance by the transformation of a problem into a great advantage.

A literature review reveals a lack of systematic studies on carbons from winery solid wastes. Most data reported on carbons from grape residues are part of comprehensive studies to evaluate the overall potential of biomass as precursor of porous carbons. As summarized in Table 1, the majority of grapes based-carbons are produced by multi-step processing of some

component (mostly seeds) and their application is essentially focused to the removal of pollutants from aqueous streams.

The interest of the present systematic approach concentrates in highlighting the potential of each single waste: bagasse, stalks and the residue from the mechanical extraction of seeds oil. Firstly, the simplicity of the hydrothermal carbonization for the generation of carbon-enriched materials raises the possibility of using this technology for minimizing the polluting impact of the winery solid residues. Secondly, the success of a simple one-step activation by CO_2 or KOH provides a second chance to these feedstocks by means of advanced environmental applications such as CO_2 capture and supercapacitors.

Despite their different origin and structure, the present solid wastes generated in wine production closely resemble with respect to hydrothermal carbonization and activation, thus allowing their management, stabilization and valorization all together, without a significant effect on the final product.

2. Materials and Methods

2.1. Raw materials

Three different wastes generated in local wineries at the Northwest of Spain have been studied: i) bagasse made of skins and seeds (B), ii) stalks (R) and iii) defatted-seeds (S). The latter were supplied as small cylindrical monoliths resulting from seeds extrusion to extract oil.

2.2. Synthesis of hydrochars

The bagasse and the stalks were used as received while oil free-seed monoliths were milled to a particle size ≤ 1 mm prior to the experiments. 10 g of residues were subjected to hydrothermal carbonization at 200 ºC in the presence of 10 g of water in a Teflon liner

stainless steel autoclave under autogenous pressure for 12 hours. The solid product was filtered, washed with 100 ml of water and dried at 100 °C for 24 h. The resulting hydrochars were named using H after the corresponding raw precursor acronym (BH, RH and SH).

2.3. Synthesis of porous carbons

2.3.1. Physical activation

Samples (previously dried and ground below 1 mm) were placed in a double-jacket quartz reactor and, heat treated in CO_2 (370 ml/ min) up to 800ºC during 30 min. The heating rate was 5 °C/min. The resulting materials are denoted as X(H)AC where X refers to the feedstock and H applies to the respective hydrochar.

2.3.2. Chemical activation

Samples were thoroughly ground with KOH (KOH/sample = 2, by weight) and heated at 5°C/min up to 800 °C under N_2 (72 ml/min) and held for 1 h. The solids were washed with HCl (10 wt%) to remove any inorganic salt and with boiling distilled water until conductivity less than 2 μS^{-1}. Finally, they were dried in an air oven at 100 °C for 24 h. The obtained carbons are designated as X(H)AK, X referring to the feedstock and H applying to the respective hydrochar.

2.4. Materials characterization

The assessment of the biochemical composition of the different feedstocks involved a previous treatment of the samples sized to 250-500 µm in a Soxhlet extractor with acetone for 8 h and, subsequently, with distilled water for 4 h. The resulting free extractive-biomass was dried in air at 60 °C to a moisture content below 15%. The contents of lignin and cellulose were determined following TAPPI standard methods, respectively, T222om-02 and T212om-02. The Browning Method (Schuerch, 1968) was used for holocellulose assessment. The

amount of hemicellulose was estimated from the difference between the contents of holocellulose and cellulose (Pettersen, 1984).

The morphology of the samples was examined by Scanning Electron Microscopy (SEM) using a Carl Zeiss DMS-942 microscope.

The chemical characteristics of the diverse materials were determined by different techniques. Thermogravimetric runs (Setaram TGA24) at 100 °C in air flow provided the moisture of the different samples. Subsequent treatment up to 815 °C for 30 min reported their ash content. Elemental analysis was carried out in a LECO CHNS-932 microanalyser provided with a LECO VTF-900 accessory for oxygen. Temperature programmed desorption (TPD) analysis entailed sample heating from 20 to 1000 °C at 15 °C/min under 50 cm^3/min Ar flow (Setaram TGA92 coupled to mass spectrometer OmnistarTM-Pfeiffer Vacuum). TPD curves were fitted with GaussianAmp peaks and the evolution of CO and CO_2 was semi-quantitatively determined using calcium oxalate as standard.

Textural features of the carbons were obtained by physical adsorption of N_2 at 77 K (Micromeritics ASAP 2010) and CO_2 at 273 K (Micromeritics TriStar 3000). "Although the limited validity of the BET equation for the characterization of microporous adsorbents has been widely addressed (Centeno and Stoeckli, 2010; ISO [International Organization for Standardization], 2010; Thommes et al., 2015; Tian and Wu, 2018), it is still the most widely used approach for determining the specific surface area of porous carbons. In a first approximation, the N_2 isotherm was analyzed by this method following the recommendations of Rouquérol et al. (Rouquerol et al., 2007) and the equivalent BET-surface area (S_{BET}) is included exclusively for comparison purposes".

The systematic analysis of N_2 isotherms by the simultaneous use of several approaches including QSDFT model (Quantachrome software package), Kaneko´s comparison plot and Dubinin´s theory allowed to get more reliable information on the specific surface area (S_{N2}) and other various porosity features (total pore volume (V_{pores}), micropore volume ($W_{o\text{-}N2}$) and average micropore width ($L_{o\text{-}N2}$) (Centeno and Stoeckli, 2010). Complementary information on the ultramicroporosity (S_{CO2}, $W_{o\text{-}CO2}$, $L_{o\text{-}CO2}$) was obtained by the analysis of CO_2 isotherm by the NLDFT approach and the Dubinin-Raduskevich equation. The pore size distributions (PSD) were obtained from the NLDFT-analysis of CO_2 isotherm combined with the QSDFT-data from N_2 adsorption.

2.5. Applications of the activated carbons

2.5.1. Adsorbents for CO_2 capture

The Dubinin´s theory allowed the calculation of the theoretical equilibrium CO_2 uptakes under post- and pre-combustion conditions (1 and 20 atm, respectively, and 298 K) using the characteristic energy (E_o) and the micropore volume (W_o) obtained from the analysis of CO_2 and N_2 adsorption isotherms (Martín et al., 2010). For some selected carbons, CO_2 capture capacities at both the atmospheric (Setaram TGA2) and high (magnetic suspension balance Rubotherm-VTI) pressures were experimentally confirmed by the maximum mass increase of the sample when exposed to a pure CO_2 atmosphere.

2.5.2. Supercapacitor electrodes

Two electrodes separated by a glassy fibrous material (Wathman 934-AH) were assembled in a Swagelok cell (8 mm in diameter). The system was subjected to galvanostatic charging-discharging cycles at 1 mA/cm^2 (Autolab-Ecochimie PGSTAT 30), the voltage ranging from 0 to 1 V in the aqueous 2 M H_2SO_4 electrolyte and between 0 and 3.5 V in the ionic liquid 1-

Ethyl-3-methylimidazolium bis(trifluoromethylsulfonyl)imide dissolved in acetonitrile (weight ratio 1:1, EMImBF_4/AN). The electrodes consisted of 90 wt.% of carbon, 5 wt.% of polytetrafluoroethylene (PTFE) and 5 wt.% of carbon black.

The gravimetric capacitance was calculated according to $C = 2I/m(dV/dt)$ where I is the current, dV/dt is the slope of the discharge curve and m is the mass of carbon in one electrode. Therefore, all capacitance values refer to a single electrode.

3. Results and discussion

3.1. Characteristics of the winery wastes

As reported by Table 2, the present feedstocks (bagasse, stalks and oil free-seeds) are composed of the three primary fractions of lignocellulosic materials (Kambo and Dutta, 2015). The content of cellulose ranges between 10 and 17 wt.%. The stiff cellulose fibrils are hold by 12-24 wt.% of hemicellulose. The presence of 33-40 wt.% of lignin retains all components strongly intermeshed. There is no statistically significant difference in the biopolymer percentages of oil free-seeds and bagasse whereas the lignin/saccharides ratio in stalks (1.8) is double than in the other wastes (~ 0.9).

These biomass residues also include 23-33 wt.% of a variety of non-structural sugars, proteins, waxes, etc. soluble in water and ethanol (extractives) and a low amount of inorganic compounds. The latter accounts for 6 wt.% in the current bagasse and stalks although it may depend on the contamination during harvesting. Oil free-seeds display somewhat higher purity with around 3 wt.% of ashes.

The set of winery feedstocks displays a similar elemental composition (Table 3) which also fits into the standard values for biomass (Gollakota et al., 2016).

The comparable profiles of CO_2 and CO release in TPD experiments (Fig. 1) suggest that the chemical nature of the surface is virtually the same for all wastes. Thus, the two peaks dominating the CO_2 evolution at around 360 °C and 650 °C are indicative of weak acidic carboxylic- and lactones-groups, respectively (Zielke et al., 1996). The temperatures at which a remarkable CO release occurs reveal the presence of α-substituted ketones and/or aldehydes (~ 350 °C), phenolic groups (670-700 °C) and chromenes and pyrones (980- 1050 °C) (Figueiredo et al., 2007). The additional peak centered at 830 °C corresponds to carbonyl and/or quinones in the oil free-seeds surface (Figueiredo et al., 2007). The integration of the TPD curves reports somewhat lower content of surface oxygenated-functionalities in oil-free seeds (Table 3).

3.2. Features of the hydrochars

Taking advantage of the high humidity of bagasse and stalks, a mild hydrothermal carbonization at 200 ºC results really attractive for their management. Both wastes are available with a moisture of around 60 wt.%, which means that they contain around 1.5 times the amount of water (by weight) with respect to dry material. The penalty is not so relevant for oil-free seeds with a humidity of around 10 wt.%.

Without prior energy consumption, the HTC processing of the winery residues minimizes the polluting impact of their rapid degradation in air by stabilizing them in partially carbonized products. Table 3 shows that the carbon content is increased up to around 67% (on a dry-ash-free basis (d.a.f.)) from 47-55% of the raw biomass whereas oxygen content is decreased by 35-40%.

The evolution of the atomic H/C and O/C ratios in a Van Krevelen diagram (Van Krevelen, 1950) indicates that hydrothermal treatment results in dehydration and decarboxylation

reactions via the removal of low molecular weight compounds (Fig. 2). These variations are consistent with the formation of a well-condensed structure observed for other hydrochars (Wiedner et al., 2013).

In view of the similar bio-composition of oil free-seeds and bagasse (Table 2), their HTC processing was expected to provide comparable yields. However, it results more efficient for the former since 72% of SH is obtained whereas BH accounts for 54% of the raw bagasse. On the other hand, the higher lignin/saccharides ratio in stalks has not impact and the yield remains at around 57% for RH. The lack of a direct correspondence with the basic trend found for the HTC throwput of the single components, lignin > cellulose > hemicellulose, suggests that interactions between biopolymers take place (Kang et al., 2012).

The mild hydrothermal carbonization is an effective way to increase the turnover time of the carbon contained in the winery residues. The C recovery is 89% for the oil free-seeds, 79% for the stalks and 70% for the bagasse. For comparison, the biochar obtained by high-temperature pyrolysis (~600°C) of oil free-seeds retains only 50% of the initial carbon content.

The ability of HTC to transfer water-soluble inorganic components of the biomass to the liquid phase is an additional advantage of this technology. As observed in Table 3, hydrothermal treatment applied on the three winery wastes leads to carbon enriched-materials with only about 3% of ash. This is not possible in the case of dry carbonization, the percentage being as high as 7% in the biochar resulting from oil free-seeds at 600 ºC. Such a reduction in ash content would become highly advantageous for further applications of the materials.

With the exception of additional peroxide- and carbonyl/quinones-groups in SH (as indicated by, respectively, CO_2 desorption at around 550 °C and CO release at 810 °C), the deconvolution of the TPD profiles suggests quite similar functionalities in the surface of the hydrochars to those detected in the initial biomass. The CO_2 evolution (Fig. 1) reports that weak acidic carboxylic and lactones groups still remain after HTC although the amount is somewhat reduced (Table 3). Additionally, the shifting of the peaks towards slightly higher temperatures reveals the formation of more stable bonds and changes in the electronic environment of the surface groups already existing in the feedstocks. Such effect is more remarkable for the O-functionalities desorbing as CO. The increase in their total amount (Table 3) likely indicates that the removal of CO_2 may also involve secondary reactions originating surface complex (C[O]) and free CO (Figueiredo et al., 2007).

SEM images (Fig. 3) evidence that structural scaffolds of the winery residues are mostly preserved by HTC. The hydrochars particles virtually maintain the original cell morphology although with less defined shape as a consequence of volatiles release. The presence of microspheres, so characteristic in saccharides derived-hydrochars (Jain et al., 2016), is observed in the bagasse-hydrochar but hardly detected in those from the other feedstocks. Very likely, they are mostly generated from the sugars left after the must extraction. Hemicellulose may also contribute somewhat to the generation of globular carbon items since its decomposition starts at ~175 ºC. A relevant contribution from the more polymerized cellulose, which degrades above 220-250 ºC, is practically excluded (Donar et al., 2016; Pala et al., 2014).

Hydrochars from winery residues present no relevant porosity accessible to N_2 at 77 K (Fig. S1) and the S_{N2} of around 24 m^2/g for BH and RH and 9 m^2/g of the seeds-hydrochar correspond to the typical low values reported for similar materials (Jain et al., 2016).

However, the complementary use of CO_2 adsorption at 273 K (Fig. S1) reveals a structure formed by ultramicropores with size < 0.8-0.9 nm (Lozano-Castelló et al., 2004) which leads to S_{CO2} of 204, 98 and 64 m^2/g for BH, RH and SH, respectively.

In summary, despite their different origin and structure, all present feedstocks closely resemble with respect to hydrothermal carbonization, thus allowing their management and stabilization all together, without a significant effect on the final product.

3.3. Characteristics of the activated carbons

The combination of diverse techniques leads to some general patterns for the activation of winery wastes. Table 3 illustrates the activation impact on the chemical composition, a significant increase in carbon content above 84% accompanied by a drop in oxygen to values between 5 and 14 wt.% taking place. The process generates a highly condensed chemical structure (Fig. 2), notably reduced in surface oxygenated groups (Table 3). It is noteworthy the similarity of the surface chemistry of all activated carbons, mainly consisting of carboxylic-, lactone- and carbonyl/quinone-groups. Pyrone and chromene-functionalities are also present in CO_2-activated carbons (Table S1).

Regardless of the precursor and activating agent, N_2 adsorption isotherms are type I (Fig. S2), indicative of an essentially microporous network. The pore size distributions (PSD) confirm a major contribution from pores below 1 nm (Fig. 4).

In spite of some common features, a more detailed study shows remarkable distinctions between the sets synthesised by physical or chemical activation.

3.3.1. Physical activation

The simple heating of dry bagasse and oil-free seeds in CO_2 at 800 °C for only 30 min maintains the cellular structure (Fig. 3) while generating porous carbons with extremely

narrow PSDs (Fig. 4). In spite of the limited porous volume (Fig. S2), such network development is virtually dominated by ultramicropores of 0.53-0.60 nm in average size (Table 4) and results in surface areas S_{CO2} as high as 979 m^2/g for BAC and 819m^2/g for SAC. In the present case, S_{BET} (which reflects the area equivalent to the total volume adsorbed) is misleading as the remarkable presence of pores below 0.8 nm causes the BET method to underrate the total surface area (Centeno and Stoeckli, 2010). The fact that the actual surface area $S_{N2,}$ estimated by the combination of different methods (Centeno and Stoeckli, 2010) is smaller than S_{CO2}, reflects the difficulties of N_2 at 77K to access to the extremely small porosity (Lozano-Castelló et al., 2004). Anyway, the comparison with values of Table 1 shows that the present one-pot activation by CO_2 competes favorably with other multi-stage physical activation previously used on winery wastes.

Contrary to the success with bagasse and seeds, the direct physical activation clearly fails on stalks. The yield of the process is only 9 wt% and 42.4 wt.% of the resulting material corresponds to ashes. It appears that the higher proportion of lignin in the intracellular matrix of stalks acts as a protective barrier and the particles are burned instead of activated (Suhas et al., 2007). In fact, the resulting RAC is mainly formed by fibers with a specific surface limited to ~ 200 m^2/g.

Taking into account the relevance of the materials purity for advanced applications, physical activation would require a subsequent acid-treatment. As illustrated by Table 3, only the material derived from oil free-seeds with 9 wt% of ash would achieve an actual potential while 17 wt% in the bagasse-activated carbon restricts its direct use in some fields. On this regard, the partial solubilization of the inorganic components that takes place during HTC becomes highly advantageous for subsequent physical activation.

Thus, a prior hydrothermal treatment on oil-free seeds successfully leads to an activated carbon (SHAC) with 50% less impurities (Table 3) and 20% higher surface (Table 4). In the case of bagasse, the pre-HTC has a major effect on the reduction of impurities to 6.5% in BHAC. The slight decrease in both the volume $W_{o\text{-}CO2}$ and the average micropores size $L_{o\text{-}CO2}$ only affect the total surface S_{CO2} by -7% with respect to BAC obtained without previous HTC.

HTC results to be an indispensable step for producing porous carbons from stalks. The poor result obtained by their direct activation with CO_2 is notably overcome by using the corresponding hydrochar as precursor and an ultramicroporous activated carbon with 635 m^2/g and 5.2 % of ash is obtained. The hydrothermal treatment weakens the cellular matrix of the feedstock (Islam et al., 2015; Sabio et al., 2016) facilitating subsequent diffusion of the gaseous activating agent.

The effectiveness of a previous HTC goes even further by increasing the activation yield (Fig. 5) and, simultaneously, reducing significantly the oxygen functionalities (Table 3) in the CO_2-activated carbons. No significant effect on the total surface area S_{CO2} is detected although the relevant reduction in S_{N2} indicates a less accessible porous network of the materials from hydrochar.

3.3.2 Chemical activation

Winery wastes have proved to be very versatile precursors that allow obtaining a wide spectrum of porous carbons by simply selecting the activation conditions. Thus, Fig. 5, as an indicator of the effectiveness of the different treatments on winery wastes, illustrates relevant differences between the materials obtained by the physical and chemical processes while the role of the feedstock is much more limited.

Definitely, treatment with KOH generates an extraordinary development of porosity in all winery wastes, making it possible for stalks to generate porous carbons very similar to those from the other residues (Tables 3 and 4). Regardless of the feedstock, the carbon particles obtained with KOH exhibit a typical morphology characterized by a fluffly appearance with no trace of the initial cellular network (Fig. 3).

It is noteworthy that whereas the activation with CO_2 engenders pores mainly below 0.6 nm, KOH-materials also exhibit a noticeable contribution from larger pores up to 1.4 nm. Despite being KOH a harsh activating agent, the set SAK, BAK and RAK still remain entirely microporous (Fig. 4) and total pore volumes of 0.70-0.83 cm^3/g (Table 4) translate to S_{BET} as high as 1700-2050 m^2/g which exceeds the values obtained by other multi-step chemical activation processes on winery residues (Table 1). Regarding the high values of S_{BET} frequently found in highly activated carbons, it should be taken into account that it does not actually correspond to their specific surface area. The quantitative correlation found by Centeno et al. (Centeno and Stoeckli, 2010) between the actual surface S_{total}, S_{BET} and the average micropore width L_o, $S_{total} = S_{BET}/(1.2 \times L_o)$, shows that S_{BET} provides a reliable estimate of the total surface area of carbons with micropores around 0.9-1.1 nm but it overestimates the real surface for carbons with a high proportion of pores wider than 1.1 nm.

Anyway, the comprehensive textural characterization by different methods (see section 2.4) confirms the outstanding porosity of the present chemically activated carbons. Their surface area S_{N2} is around 1300-1500 m^2/g (Table 4) which approaches the highest limits of actual surface found for activated carbons (Lobato et al., 2017). In addition, the good agreement with S_{CO2} indicates that KOH activation also enhances the accessibility of the porous system of the resulting activated carbons (Fig. 4).

Regarding the surface nature, there are no remarkable differences in the density of surface [O]-groups in the KOH-activated carbons derived from S and B if compared to their homologues obtained with CO_2 (Table 3) although TPD profiles reveal higher stability of CO-functionalities (Fig. 2).

A very positive result of chemical activation is the low ash content of the carbons SAK, BAK and RAK (2-4 wt%). These values can be further reduced by a previous hydrothermal treatment, the impurities accounting for only 0.1 wt.% in BHAK (Table 3).

Fig. 5 shows how the severity of the chemical activation minimizes the influence of a prior hydrothermal carbonization. The impact of pre-HTC on the KOH-activation yield as well as on the composition of the resulting materials (Table 3), is much less obvious than that observed on physical activation. These findings are coherent with the similar morphology and texture of their counterparts with no pre-treatment. The particles of SHAK, BHAK and RHAK display the typical sponge-like morphology observed for SAK, BAK and RHAK, obtained directly from the dry feedstocks (Fig. 3). The total surface area of the KOH-activated hydrochars is 15-20% higher (Fig. 5), the PSD being barely modified (Fig. 4).

3.4 Applications

The variety of physico-chemical features of the present carbons opens their possibilities for diverse applications with high environmental impact.

3.4.1 CO_2 capture capacity

As shown below, winery wastes allow the preparation of low-cost carbon adsorbents with superior CO_2 capture in thermoelectric power plants. Following Martín et al. (2010), the suitability of the present carbons to be applied as adsorbent for CO_2 capture has been estimated. Table 5 summarizes their maximum CO_2 uptake at 1 and 20 atm (298 K), i.e. under

conditions relevant to post- and pre-combustion capture, respectively. It also includes experimental results for selected samples which confirm the accuracy of this approach.

Despite the simplicity of the one-step physical activation, the resulting materials reach post-combustion CO_2 capture of around 10-12 wt % which meet the upper-bound reported in the literature for standard activated carbons (Lee and Park, 2015; Marco-Lozar et al., 2014; Martín et al., 2010). Although they display moderate pore volumes, the ability is enhanced by their tailored porosity virtually made of pores smaller than 0.6 nm (Fig. 4).

Higher pore volumes and a wider distribution of micropores achieved by activation with KOH cause the resulting materials to surpass these values (13-16 wt%), while also being excellent for capture under pre-combustion conditions (55-69 wt%) (Marco-Lozar et al., 2014).

3.4.2 Electrochemical capacitance as electrodes in supercapacitors

Activated carbons derived from winery wastes are also worthy of attention as electrode materials for the storage of electrical energy in supercapacitors (Fig. 6). Taking advantage of the high specific surface area of the materials obtained by mild KOH activation, their electrochemical capacitance is among the highest reported for porous carbons (Lobato et al., 2017). The as-prepared materials exhibit superior specific capacitance of 262-296 F/g in the aqueous H_2SO_4. Furthermore, they also offer advantages with respect to attainable specific capacitance ranging between 142 and 179 F/g (Table 5) in the advanced electrolyte based on the ionic liquid $EMImBF_4$ (Bhoyate et al., 2017; Zhang and Zhao, 2012).

As a consequence of their attainable electrochemical capacitance, high availability, low economic value and environmental concern, they offer advantages with respect to other biomass based-carbons or more sophisticated materials.

4. Conclusions

This study supports the option to value solid winery wastes via one-pot activations. Bagasse, stalks and oil free-seeds have resulted excellent precursors for the production of low-cost sustainable porous carbons with promising commercial prospects. The particular physico-chemical features of the resulting activated carbons provided with high performance for environmental applications such as CO_2 capture processes and storage of electrical energy in supercapacitors.

Benefiting from the high humidity of the winery wastes, a mild hydrothermal carbonization resulted to be an interesting technology which minimizes the polluting impact by stabilizing them in enriched-carbon solids products and acts as a leaching process.

Aknowledgements

This study received financial support from CSIC in the frame of Project PIE-201680E035. N.Q. acknowledges a fellowship from Gobierno del Principado de Asturias (Programa Severo Ochoa). L.S. thanks the support from Programa Estatal de Promoción del Talento y su Empleabilidad en I+D+i and European Social Fund-Youth Employment Initiative.

The selfless support and winery wastes provided by Mr. Víctor Alejandro Chacón (Bodega Chacón Buelta-Cerredo, Spain), Dr. M. Carmen Martínez (MBG-CSIC) and Mr. Carlos Ron (Bodega Vitheras-Carballo, Spain) are specially acknowledged. The authors wish to thank for supplying grape bagasse and stalks.

References

Al Bahri, M., Calvo, L., Gilarranz, M.A., Rodriguez, J.J., 2016. Diuron Multilayer Adsorption on Activated Carbon from CO_2 Activation of Grape Seeds. Chem. Eng. Commun. 203, 103–113. https://doi.org/10.1080/00986445.2014.934447

Alonso, D.M., Wettstein, S.G., Dumesic, J.A., 2012. Bimetallic catalysts for upgrading of biomass to fuels and chemicals. Chem. Soc. Rev. 41, 8075. https://doi.org/10.1039/c2cs35188a

Arvanitoyannis, I.S., Ladas, D., Mavromatis, A., 2008. Wine Waste Management : Treatment Methods Treated Waste, Waste Management for the Food Industries. Elsevier Inc. https://doi.org/10.1016/B978-0-12-373654-3.50010-9

Aurand, J.M., 2015. State of the Vitiviniculture World Market. 38th OIV World Congr. vine wine 1–14.

Bhoyate, S., Ranaweera, C.K., Zhang, C., Morey, T., Hyatt, M., Kahol, P.K., Ghimire, M., Mishra, S.R., Gupta, R.K., 2017. Eco-Friendly and High Performance Supercapacitors for Elevated Temperature Applications Using Recycled Tea Leaves. Glob. Challenges 1700063, 1700063. https://doi.org/10.1002/gch2.201700063

Brandt, A., Gräsvik, J., Hallett, J.P., Welton, T., 2013. Deconstruction of lignocellulosic biomass with ionic liquids. Green Chem. 15, 550. https://doi.org/10.1039/c2gc36364j

Bustamante, M.A., Moral, R., Paredes, C., Pérez-Espinosa, A., Moreno-Caselles, J., Pérez-Murcia, M.D., 2008. Agrochemical characterisation of the solid by-products and residues from the winery and distillery industry. Waste Manag. 28, 372–380. https://doi.org/10.1016/j.wasman.2007.01.013

Centeno, T.A., Stoeckli, F., 2010. The assessment of surface areas in porous carbons by two model-independent techniques, the DR equation and DFT. Carbon N. Y. 48, 2478–2486. https://doi.org/10.1016/j.carbon.2010.03.020

Deiana, A.C., Gimenez, M., Sardella, M.F., Sapag, K., Masseo, A.L.S., Teixeira, A.P.C., Araujoc, M.H., Lago, R.M., 2014. Catalytic oxidation of aqueous sulfide promoted by oxygen functionalities on the surface of activated carbon briquettes produced from viticulture wastes. J. Braz. Chem. Soc. 25, 2392–2398. https://doi.org/10.5935/0103-5053.20140265

Deiana, A.C., Gimenez, M.G., Rómoli, S., Sardella, M.F., Sapag, K., 2014. Batch and Column Studies for the Removal of Lead from Aqueous Solutions Using Activated Carbons from Viticultural Industry Wastes. Adsorpt. Sci. Technol. 32, 181–196. https://doi.org/10.1260/0263-6174.32.2-3.181

Deiana, A.C., Sardella, M.F., Silva, H., Amaya, A., Tancredi, N., 2009. Use of grape stalk, a waste of the viticulture industry, to obtain activated carbon. J. Hazard. Mater. 172, 13–19. https://doi.org/10.1016/j.jhazmat.2009.06.095

Demiral, H., 2016. Adsorption of copper (II) from aqueous solutions on activated carbon prepared from grape bagasse. J. Clean. Prod. 124, 103–113.

https://doi.org/10.1016/j.jclepro.2016.02.084

Devesa-Rey, R., Vecino, X., Varela-Alende, J.L., Barral, M.T., Cruz, J.M., Moldes, A.B., 2011. Valorization of winery waste vs. the costs of not recycling. Waste Manag. 31, 2327–2335. https://doi.org/10.1016/j.wasman.2011.06.001

Donar, Y.O., Çağlar, E., Sinağ, A., 2016. Preparation and characterization of agricultural waste biomass based hydrochars. Fuel 183, 366–372. https://doi.org/10.1016/j.fuel.2016.06.108

Dwyer, K., Hosseinian, F., Rod, M., 2014. The Market Potential of Grape Waste Alternatives. J. Food Res. 3, 91. https://doi.org/10.5539/jfr.v3n2p91

El Achkar, J.H., Lendormi, T., Hobaika, Z., Salameh, D., Louka, N., Maroun, R.G., Lanoisellé, J.L., 2016. Anaerobic digestion of grape pomace: Biochemical characterization of the fractions and methane production in batch and continuous digesters. Waste Manag. 50, 275–282. https://doi.org/10.1016/j.wasman.2016.02.028

Figueiredo, J.L., Pereira, M.F.R., Freitas, M.M.A., Órfão, J.J.M., 2007. Characterization of active sites on carbon catalysts. Ind. Eng. Chem. Res. 46, 4110–4115. https://doi.org/10.1021/ie061071v

Gergova, K., Petrov, N., Eser, S., 1994. Adsorption properties and microstructure of activated carbons produced from agricultural by-products by steam pyrolysis. Carbon N. Y. 32, 693–702. https://doi.org/10.1016/0008-6223(94)90091-4

Gollakota, A.R.K., Kishore, N., Gu, S., 2016. A review on hydrothermal liquefaction of biomass. Renew. Sustain. Energy Rev. 81, 1378–1392. https://doi.org/10.1016/j.rser.2017.05.178

González-Paramás, A.M., Esteban-Ruano, S., Santos-Buelga, C., De Pascual-Teresa, S., Rivas-Gonzalo, J.C., 2004. Flavanol Content and Antioxidant Activity in Winery Byproducts. J. Agric. Food Chem. 52, 234–238. https://doi.org/10.1021/jf0348727

Güzel, F., Sayğili, H., 2016. Adsorptive efficacy analysis of novel carbonaceous sorbent derived from grape industrial processing wastes towards tetracycline in aqueous solution. J. Taiwan Inst. Chem. Eng. 60, 236–240. https://doi.org/10.1016/j.jtice.2015.10.003

Islam, M.A., Tan, I.A.W., Benhouria, A., Asif, M., Hameed, B.H., 2015. Mesoporous and adsorptive properties of palm date seed activated carbon prepared via sequential hydrothermal carbonization and sodium hydroxide activation. Chem. Eng. J. 270, 187–195. https://doi.org/10.1016/j.cej.2015.01.058

ISO [International Organization for Standardization], 2010. Determination of the specific surface area of solids by gas adsorption - BET method (ISO 9277:2010(E)). Ref. number ISO 9277, 30 pp. https://doi.org/10.1007/s11367-011-0297-3

Jain, A., Balasubramanian, R., Srinivasan, M.P., 2016. Hydrothermal conversion of biomass waste to activated carbon with high porosity: A review. Chem. Eng. J. 283, 789–805. https://doi.org/10.1016/j.cej.2015.08.014

Jimenez-Cordero, D., Heras, F., Alonso-Morales, N., Gilarranz, M.A., Rodriguez, J.J., 2015. Ozone as oxidation agent in cyclic activation of biochar. Fuel Process. Technol. 139, 42–48. https://doi.org/10.1016/j.fuproc.2015.08.016

Jimenez-Cordero, D., Heras, F., Alonso-Morales, N., Gilarranz, M.A., Rodríguez, J.J., 2014. Preparation of granular activated carbons from grape seeds by cycles of liquid phase oxidation and thermal desorption. Fuel Process. Technol. 118, 148–155. https://doi.org/10.1016/j.fuproc.2013.08.019

Jimenez-Cordero, D., Heras, F., Alonso-Morales, N., Gilarranz, M.A., Rodriguez, J.J., 2013. Development of porosity upon physical activation of grape seeds char by gas phase oxygen chemisorption-desorption cycles. Chem. Eng. J. 231, 172–181. https://doi.org/10.1016/j.cej.2013.07.005

Kambo, H.S., Dutta, A., 2015. A comparative review of biochar and hydrochar in terms of production, physico-chemical properties and applications. Renew. Sustain. Energy Rev. https://doi.org/10.1016/j.rser.2015.01.050

Kang, S., Li, X., Fan, J., Chang, J., 2012. Characterization of hydrochars produced by hydrothermal carbonization of lignin, cellulose, d-xylose, and wood meal. Ind. Eng. Chem. Res. 51, 9023–9031. https://doi.org/10.1021/ie300565d

Lee, S.Y., Park, S.J., 2015. A review on solid adsorbents for carbon dioxide capture. J. Ind. Eng. Chem. 23, 1–11. https://doi.org/10.1016/j.jiec.2014.09.001

Lobato, B., Suárez, L., Guardia, L., Centeno, T.A., 2017. Capacitance and surface of carbons in supercapacitors. Carbon N. Y. 122, 434–445. https://doi.org/10.1016/j.carbon.2017.06.083

Lozano-Castelló, D., Cazorla-Amorós, D., Linares-Solano, A., 2004. Usefulness of CO2 adsorption at 273 K for the characterization of porous carbons. Carbon N. Y. 42, 1231–1236. https://doi.org/10.1016/j.carbon.2004.01.037

Lucian, M., Fiori, L., 2017. Hydrothermal carbonization of waste biomass: Process design,

modeling, energy efficiency and cost analysis. Energies 10, 1–5. https://doi.org/10.3390/en10020211

Mäkelä, M., Kwong, C.W., Broström, M., Yoshikawa, K., 2017. Hydrothermal treatment of grape marc for solid fuel applications. Energy Convers. Manag. 145, 371–377. https://doi.org/10.1016/j.enconman.2017.05.015

Marco-Lozar, J.P., Kunowsky, M., Suárez-García, F., Linares-Solano, A., 2014. Sorbent design for CO2 capture under different flue gas conditions. Carbon N. Y. 72, 125–134. https://doi.org/10.1016/j.carbon.2014.01.064

Martín, C.F., Plaza, M.G., Pis, J.J., Rubiera, F., Pevida, C., Centeno, T.A., 2010. On the limits of CO2 capture capacity of carbons. Sep. Purif. Technol. 74, 225–229. https://doi.org/10.1016/j.seppur.2010.06.009

Martínez, N.D., Venturini, R.B., Silva, H.S., González, J.E., Rodríguez, A.M., 2009. Copper on activated carbon for catalytic wet air oxidation. Mater. Res. 12, 45–50.

Mechati, F., Bouchelta, C., Medjram, M.S., Benrabaa, R., Ammouchi, N., 2015. Effect of hard and soft structure of different biomasses on the porosity development of activated carbon prepared under N<inf>2</inf>/microwave radiations. J. Environ. Chem. Eng. 3, 1928–1938. https://doi.org/10.1016/j.jece.2015.07.007

Mena, I.F., Diaz, E., Rodriguez, J.J., Mohedano, A.F., 2017. CWPO of bisphenol A with iron catalysts supported on microporous carbons from grape seeds activation. Chem. Eng. J. 318, 153–160. https://doi.org/10.1016/j.cej.2016.06.029

Muhlack, R.A., Potumarthi, R., Jeffery, D.W., 2017. Sustainable wineries through waste valorisation: A review of grape marc utilisation for value-added products. Waste Manag. https://doi.org/10.1016/j.wasman.2017.11.011

O'Grady, M.N., Carpenter, R., Lynch, P.B., O'Brien, N.M., Kerry, J.P., 2008. Addition of grape seed extract and bearberry to porcine diets: Influence on quality attributes of raw and cooked pork. Meat Sci. 78, 438–446. https://doi.org/10.1016/j.meatsci.2007.07.011

Okman, I., Karagöz, S., Tay, T., Erdem, M., 2014. Activated carbons from grape seeds by chemical activation with potassium carbonate and potassium hydroxide. Appl. Surf. Sci. 293, 138–142. https://doi.org/10.1016/j.apsusc.2013.12.117

Özçimen, D., Ersoy-Meriçboyu, A., 2009. Removal of copper from aqueous solutions by adsorption onto chestnut shell and grapeseed activated carbons. J. Hazard. Mater. 168, 1118–1125. https://doi.org/10.1016/j.jhazmat.2009.02.148

Ozdemir, I., Şahin, M., Orhan, R., Erdem, M., 2014. Preparation and characterization of activated carbon from grape stalk by zinc chloride activation. Fuel Process. Technol. 125, 200–206. https://doi.org/10.1016/j.fuproc.2014.04.002

Pala, M., Kantarli, I.C., Buyukisik, H.B., Yanik, J., 2014. Hydrothermal carbonization and torrefaction of grape pomace: A comparative evaluation. Bioresour. Technol. 161, 255–262. https://doi.org/10.1016/j.biortech.2014.03.052

Pettersen, R.C., 1984. The Chemical Composition of Wood, in: The Chemistry of Solid Wood, Advances in Chemistry. American Chemical Society, pp. 2–57. https://doi.org/doi:10.1021/ba-1984-0207.ch002

Rouquerol, J., Llewellyn, P., Rouquerol, F., 2007. Is the bet equation applicable to microporous adsorbents? 2991, 49–56. https://doi.org/10.1016/S0167-2991(07)80008-5

Ruiz, B., Ruisánchez, E., Gil, R.R., Ferrera-Lorenzo, N., Lozano, M.S., Fuente, E., 2015. Sustainable porous carbons from lignocellulosic wastes obtained from the extraction of tannins. Microporous Mesoporous Mater. 209, 23–29. https://doi.org/10.1016/j.micromeso.2014.09.004

Sabio, E., Álvarez-Murillo, A., Román, S., Ledesma, B., 2016. Conversion of tomato-peel waste into solid fuel by hydrothermal carbonization: Influence of the processing variables. Waste Manag. 47, 122–132. https://doi.org/10.1016/j.wasman.2015.04.016

Sardella, F., Gimenez, M., Navas, C., Morandi, C., Deiana, C., Sapag, K., 2015. Conversion of viticultural industry wastes into activated carbons for removal of lead and cadmium. J. Environ. Chem. Eng. 3, 253–260. https://doi.org/10.1016/j.jece.2014.06.026

Savova, D., Apak, E., Ekinci, E., Yardim, F., Petrov, N., Budinova, T., Razvigorova, M., Minkova, V., 2001. Biomass conversion to carbon adsorbents and gas. Biomass and Bioenergy 21, 133–142. https://doi.org/10.1016/S0961-9534(01)00027-7

Sayğili, H., Güzel, F., 2015. Performance of new mesoporous carbon sorbent prepared from grape industrial processing wastes for malachite green and congo red removal. Chem. Eng. Res. Des. 100, 27–38. https://doi.org/10.1016/j.cherd.2015.05.014

Sayğili, H., Güzel, F., Önal, Y., 2015. Conversion of grape industrial processing waste to activated carbon sorbent and its performance in cationic and anionic dyes adsorption. J. Clean. Prod. 93, 84–93. https://doi.org/10.1016/j.jclepro.2015.01.009

Schuerch, C., 1968. Methods of wood chemistry. vol. II. B. L. Browning, Ed., Wiley, New York, 1967. 498 pp. $18.75. J. Polym. Sci. Part A-2 Polym. Phys. 6, 1943–1944.

https://doi.org/10.1002/pol.1968.160061112

Suhas, Carrott, P.J.M., Ribeiro Carrott, M.M.L., 2007. Lignin - from natural adsorbent to activated carbon: A review. Bioresour. Technol. 98, 2301–2312. https://doi.org/10.1016/j.biortech.2006.08.008

Szymánski, G.S., Karpi´nski, Z., Biniak, S., Swiatkowski, A., 2002. The effect of the gradual thermal decomposition of surface oxygen species on the chemical and catalytic properties of oxidized activated carbon. Carbon N. Y. 40, 2627–2639. https://doi.org/10.1016/S0008-6223(02)00188-4

Thommes, M., Kaneko, K., Neimark, A. V., Olivier, J.P., Rodriguez-Reinoso, F., Rouquerol, J., Sing, K.S.W., 2015. Physisorption of gases, with special reference to the evaluation of surface area and pore size distribution (IUPAC Technical Report). Pure Appl. Chem. 87, 1051–1069. https://doi.org/10.1515/pac-2014-1117

Tian, Y., Wu, J., 2018. A comprehensive analysis of the BET area for nanoporous materials. AIChE J. 64, 286–293. https://doi.org/10.1002/aic.15880

Titirici, M.-M., White, R.J., Brun, N., Budarin, V.L., Su, D.S., del Monte, F., Clark, J.H., MacLachlan, M.J., 2015. Sustainable carbon materials. Chem. Soc. Rev. 44, 250–290. https://doi.org/10.1039/C4CS00232F

Toscano, G., Riva, G., Duca, D., Pedretti, E.F., Corinaldesi, F., Rossini, G., 2013. Analysis of the characteristics of the residues of the wine production chain finalized to their industrial and energy recovery. Biomass and Bioenergy 55, 260–267. https://doi.org/10.1016/j.biombioe.2013.02.015

Tsoncheva, T., Velinov, N., Ivanova, R., Stoycheva, I., Tsyntsarski, B., Spassova, I., Paneva, D., Issa, G., Kovacheva, D., Genova, I., Mitov, I., Petrov, N., 2015. Formation of catalytic active sites in iron modified activated carbons from agriculture residues. Microporous Mesoporous Mater. 217, 87–95. https://doi.org/10.1016/j.micromeso.2015.06.008

Van Krevelen, D., 1950. Graphical statistical method for the study of structure and reaction processes of coal.

Wiedner, K., Rumpel, C., Steiner, C., Pozzi, A., Maas, R., Glaser, B., 2013. Chemical evaluation of chars produced by thermochemical conversion (gasification, pyrolysis and hydrothermal carbonization) of agro-industrial biomass on a commercial scale. Biomass and Bioenergy 59, 264–278. https://doi.org/10.1016/j.biombioe.2013.08.026

Yedro, F.M., García-Serna, J., Cantero, D.A., Sobrón, F., Cocero, M.J., 2015. Hydrothermal fractionation of grape seeds in subcritical water to produce oil extract, sugars and lignin. Catal. Today 257, 160–168. https://doi.org/10.1016/j.cattod.2014.07.053

Zhang, J., Zhao, X.S., 2012. On the configuration of supercapacitors for maximizing electrochemical performance. ChemSusChem 5, 818–841. https://doi.org/10.1002/cssc.201100571

Zhang, N., Hoadley, A., Patel, J., Lim, S., Li, C., 2017. Sustainable options for the utilization of solid residues from wine production. Waste Manag. 60, 173–183. https://doi.org/10.1016/j.wasman.2017.01.006

Zhu, Y., Murali, S., Stoller, M.D., Ganesh, K.J., Cai, W., Ferreira, P.J., Pirkle, A., Wallace, R.M., Cychosz, K.A., Thommes, M., Su, D., Stach, E.A., Ruoff, R.S., 2011. Carbon-Based Supercapacitors Produced by Activation of Graphene. Science (80-.). 332, 1537 LP-1541.

Zielke, U., Huttinger, K.J., Hoffman, W.P., 1996. Surface-oxidized carbon fibers .1. Surface structure and chemistry. Carbon N. Y. 34, 983–998. https://doi.org/10.1016/0008-6223(96)00032-2

Table Captions

Table 1. Summary of activated carbons obtained from winery wastes.

Table 2. Composition of winery wastes (wt% dry basis).

Table 3. Elemental analysis and surface oxygenated groups determined by TPD of feedstocks, hydrochars and activated carbons.

Table 4. Porosity features of the activated carbons derived from winery wastes.

Table 5. CO_2 capture capacity and electrochemical capacitance of activated carbons derived from winery wastes.

Figure Captions

Figure 1. CO_2 and CO release in TPD experiments.

Figure 2. Van Krevelen diagram of raw biomass, hydrochars and activated carbons.
Inset: Relative position of the different set of samples as consequence of primary processes: demethanation (red line), dehydration (purple line) and decarboxylation (green line).

Figure 3. SEM images of the winery wastes and the corresponding hydrocarbons and activated carbons.

Figure 4. Pore size distribution in the activated carbons derived from winery residues. NLDFT analysis of CO_2 adsorption (-----) and QSDFT analysis of N_2 adsorption (- - -) are combined.

Figure 5. Correlation between the yield and the specific surface area for the different processes on winery wastes.

Figure 6. Galvanostatic charge-discharge curves of the supercapacitors based on carbons obtained from KOH activation of grape seeds.

Figure 1.

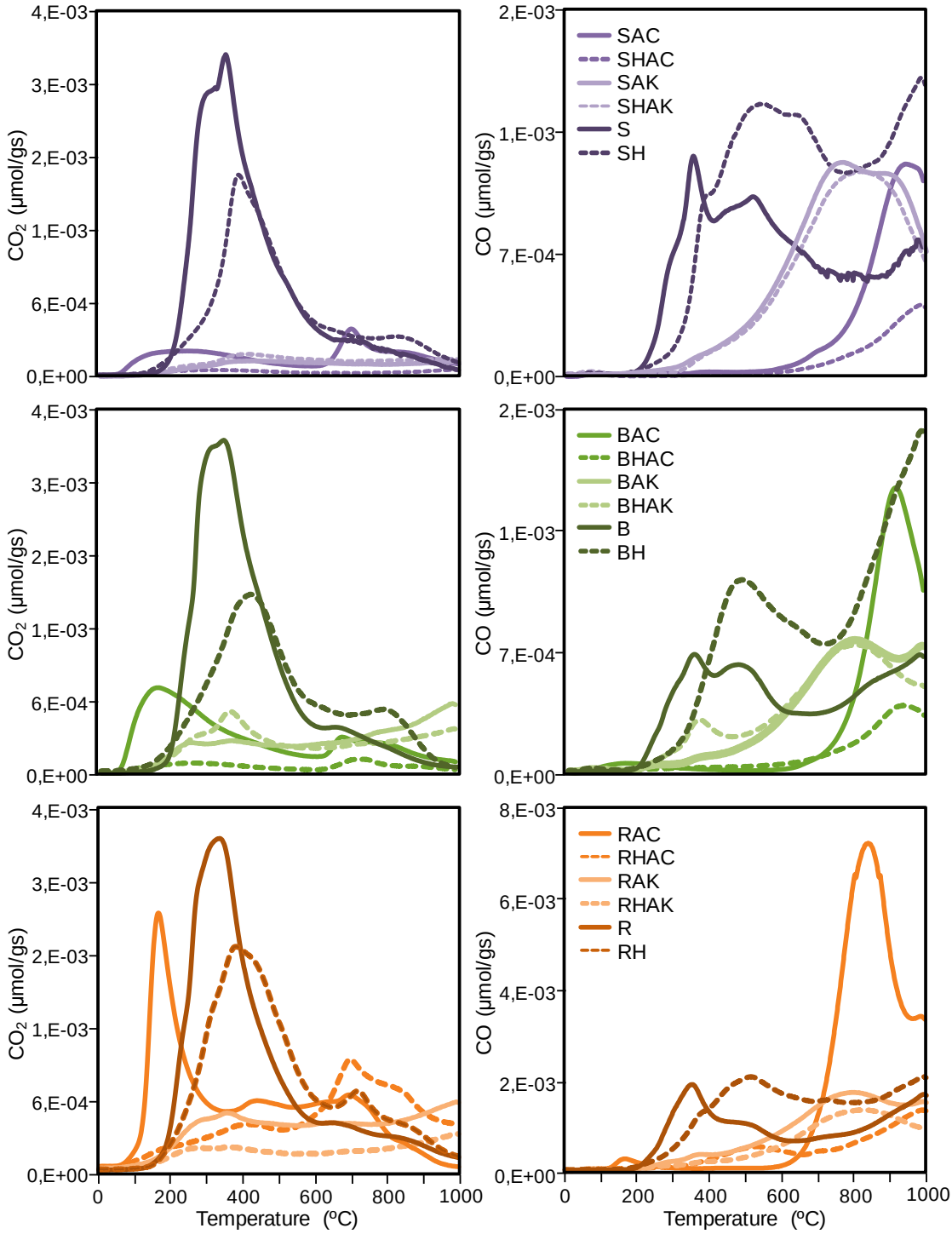
4,E-03
3,E-03
2,E-03
1,E-03
6,E-04
0,E+00
CO2 (µmol/gs)
2,E-03
1,E-03
7,E-04
0,E+00
CO (µmol/gs)
SAC
SHAC
SAK
SHAK
S
SH
BAC
BHAC
BAK
BHAK
B
BH
8,E-03
6,E-03
4,E-03
RAC
RHAC
RAK
RHAK
R
RH
0
200
400
600
800
1000
Temperature (ºC)

Figure 2.

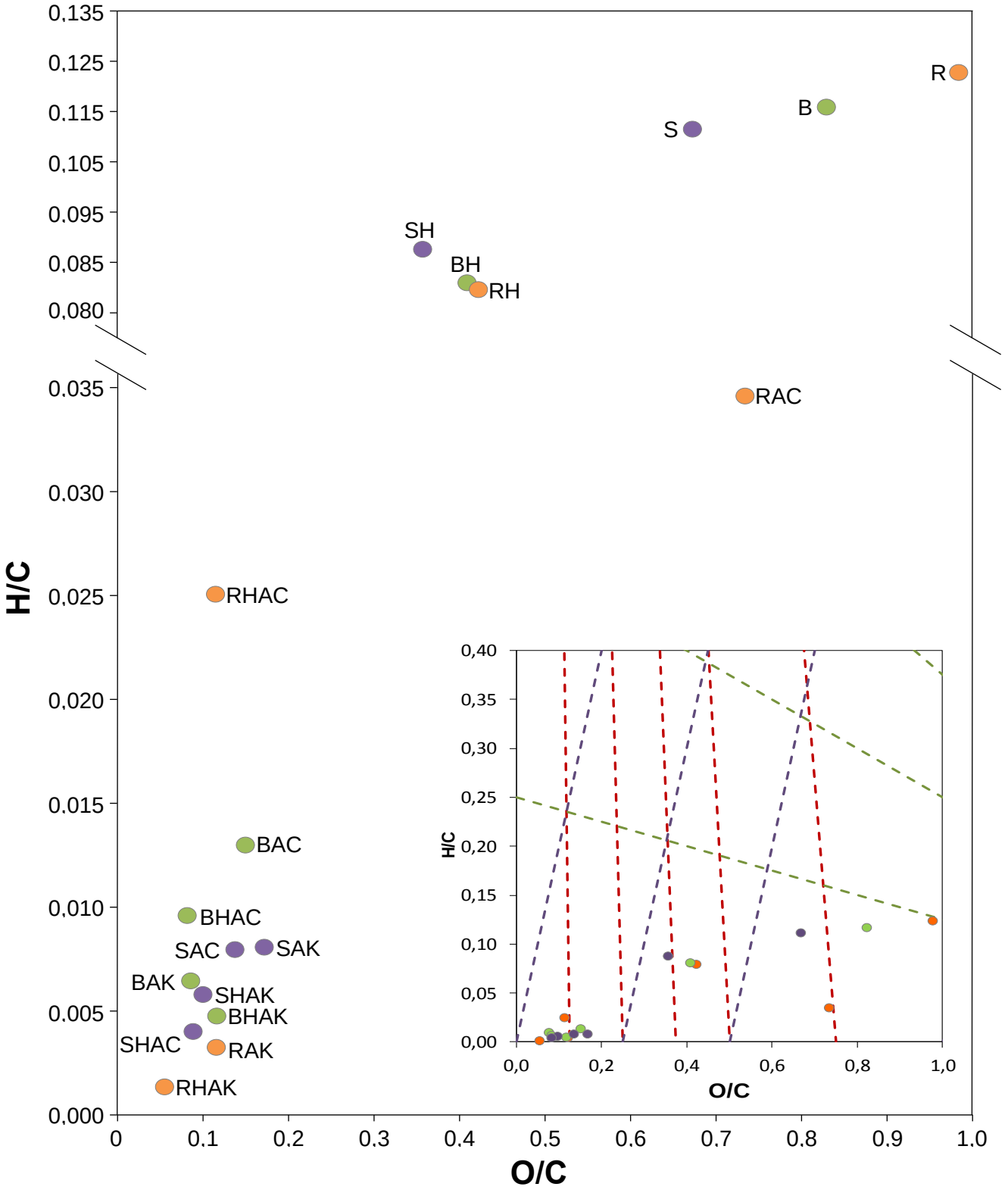
H/C
O/C
0,135
0,125
0,115
0,105
0,095
0,085
0,080
0,035
0,030
0,025
0,020
0,015
0,010
0,005
0,000
0
0.1
0.2
0.3
0.4
0.5
0.6
0.7
0.8
0.9
1.0
R
B
S
SH
BH
RH
RAC
RHAC
BAC
BHAC
SAC
SAK
BAK
SHAK
BHAK
SHAC
RAK
RHAK
0,40
0,35
0,30
0,25
0,20
0,15
0,10
0,05
0,00
0,0
0,2
0,4
0,6
0,8
1,0

Figure 3.

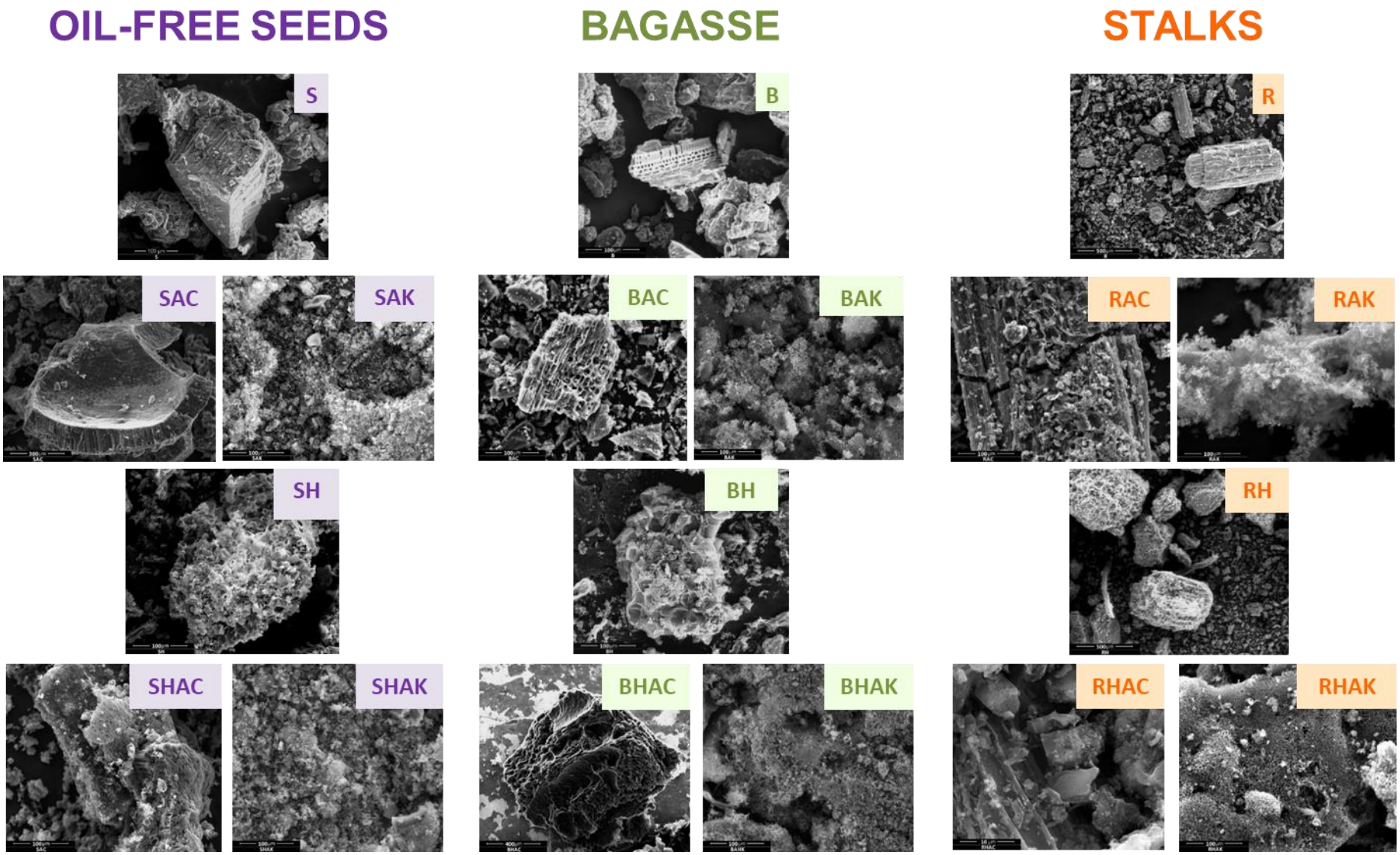
OIL-FREE SEEDS
BAGASSE
STALKS
S
B
R
SAC
SAK
BAC
BAK
RAC
RAK
SH
BH
RH
SHAC
SHAK
BHAC
BHAK
RHAC
RHAK

Figure 4.

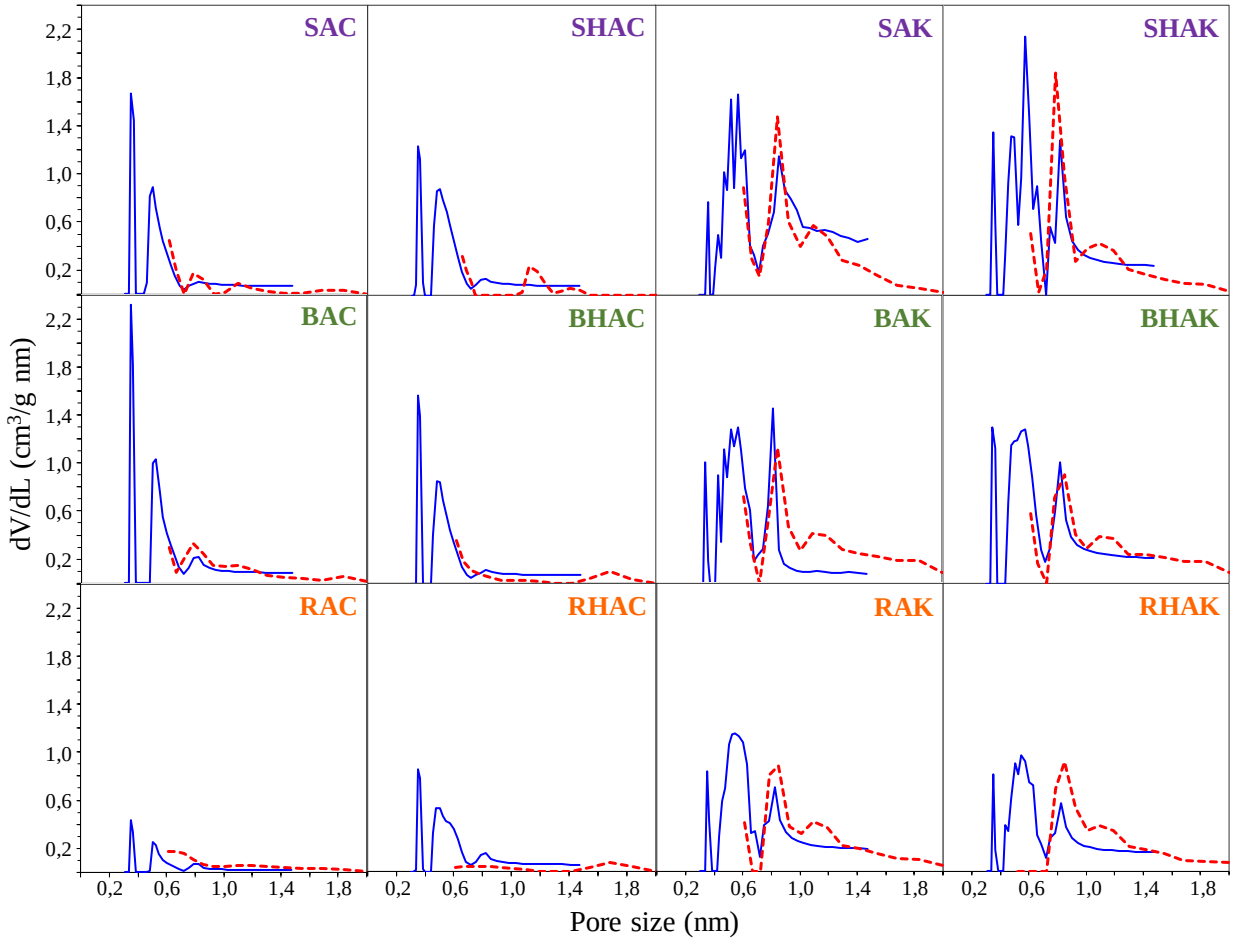
SAC
SHAC
SAK
SHAK
BAC
BHAC
BAK
BHAK
RAC
RHAC
RAK
RHAK
dV/dL (cm³/g nm)
Pore size (nm)
0,2
0,6
1,0
1,4
1,8
2,2

Figure 5.

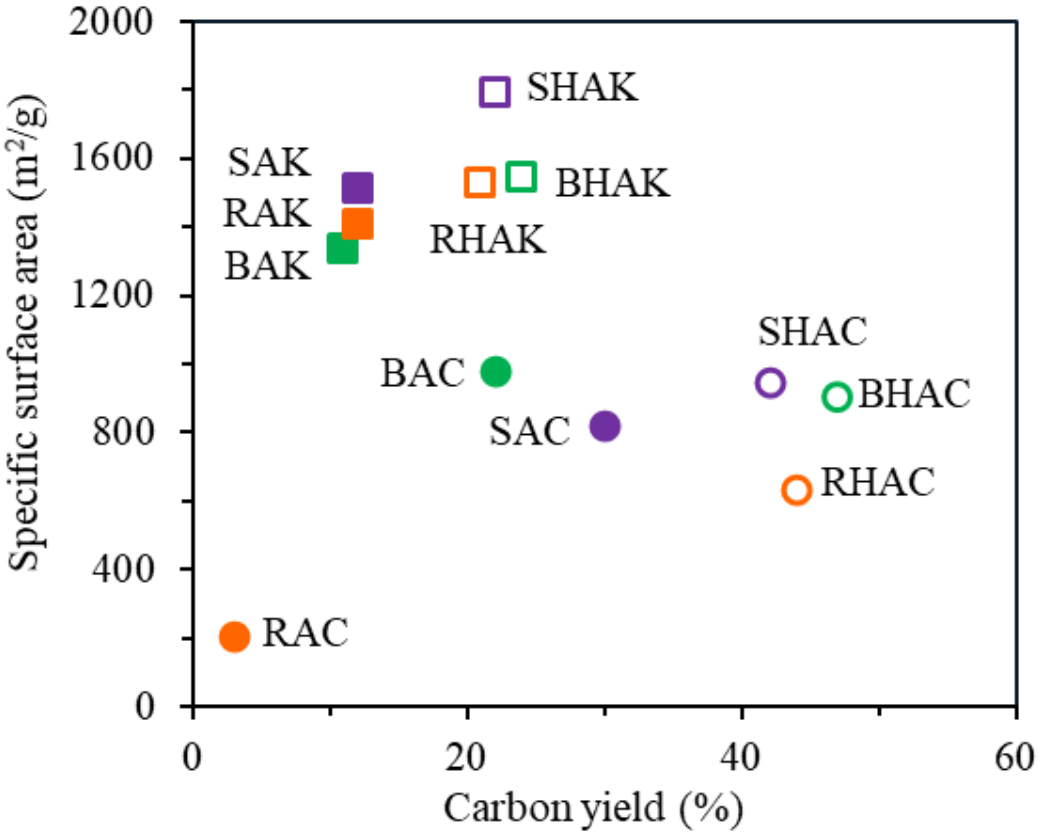
2000
1600
1200
800
400
0
Specific surface area (m²/g)
0
20
40
60
Carbon yield (%)
SHAK
SAK
RAK
BAK
BHAK
RHAK
SHAC
BHAC
BAC
SAC
RHAC
RAC

Figure 6.

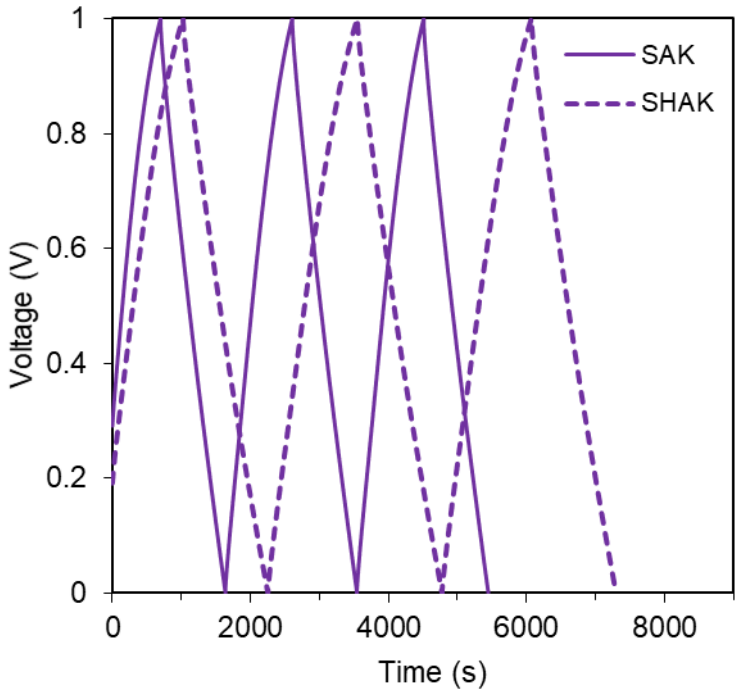

Table 1.

Precursor	Activation process	S_{BET} (m^2/g)	Application	Reference
Grape seeds	1step-Steam	497	-	(Savova et al., 2001)
Grape seeds	1 step-Steam	403	-	(Gergova et al., 1994)
Grape stalk	2 steps-Steam Prior HCl leaching	105-923	-	(Deiana et al., 2014a)
Grape stalk and pomace	2 steps-Steam Prior HCl leaching	285-923	Catalytic oxidation of aqueous sulphide Pb removal from aqueous solutions	(Deiana et al., 2014b)
Grape stalks	2 steps-Steam	846	Catalytic Wet Air Oxidation	(Martínez et al., 2009)
Grape stalk, lex and pomace	2 steps-Steam	266-798	Pb, Cd removal	(Sardella et al., 2015)
Grape seeds	2 steps-Air	440	Catalytic wet peroxide oxidation of bisphenol A	(Mena et al., 2017)
Grape seeds	2 steps-Steam	603	Formation of iron catalytic sites	(Tsoncheva et al., 2015)
Grape seeds	2 steps-CO_2	380-714	Diuron adsorption from water	(Al Bahri et al., 2016)
Grape stalk	1 step-H_3PO_4	1000-1676	-	(Deiana et al., 2009)
Grape bagasse	1 step-H_3PO_4	292-1455	Cu removal from aqueous solutions	(Demiral, 2016)
Grape seeds	2 steps H_2SO_4/H_3PO_4	657-1139	Diuron adsorption from water	(Al Bahri et al., 2012)
Residue of extraction of tannins from grape seeds	2 step-KOH	1038-1860	Adsorption of CO_2, CH_4 and H_2	(Ruiz et al., 2015)
Grape seeds	1 step-K_2CO_3/KOH	33-1238	-	(Okman et al., 2014)
Grape seeds	1 step-$ZnCl_2$	916	Cu removal from aqueous solutions	(Özçimen and Ersoy-Meriçboyu, 2009)
Grape processing wastes	1 step-$ZnCl_2$	819-1455	Cationic and anionic dyes adsorption	(Sayğili et al., 2015)

Grape pulp	1 step-$ZnCl_2$	1455	Tetracyclinein adsorption Dyes adsorption	(Güzel and Sayğili, 2016; Sayğili and Güzel, 2015)
Grape stalk	1 step-$ZnCl_2$/CO_2	211-1412	-	(Ozdemir et al., 2014)
Grape stalk	2 steps-H_2SO_4/Microwave	530	-	(Mechati et al., 2015)
Grape seeds pre-treated by hexane extraction to remove oil	Gas phase oxygen chemisorption-desorption cycles on seeds-char	1129-1256 S_{CO2}~1250	-	(Jimenez-Cordero et al., 2013)
Grape seeds pre-treated by hexane extraction to remove oil	Cycles of liquid phase oxidation and thermal desorption on seeds-char	600-1450	-	(Jimenez-Cordero et al., 2014)
Grape seeds pre-treated by hexane to remove oil	Cyclic treatments with ozone on seeds-char	350-1200 S_{CO2}~1500		(Jimenez-Cordero et al., 2015)

Table 2.

Winery waste	Cellulose	Hemicellulose	Lignin	Extractives	Ash
Oil-free Seeds (S)	14 ± 1	24 ± 4	36 ± 2	23 ± 4	3 ± 1
Bagasse (B)	17 ± 1	22 ± 2	33 ± 3	22 ± 1	6 ± 1
Stalks (R)	10 ± 1	12 ± 2	40 ± 4	33 ± 3	6 ± 1

Winery waste	Sample	Ash (wt %)	Elemental analysis (wt %, daf)				Surface oxygenated groups			
			C	H	N	O	$[CO_2]$ (μmol/g)	[CO] (μmol/g)	$[O]=2[CO_2]+[CO]$ (μmol/g)	$[O]/S_{total}$ (μmol/m^2)
Oil free-seeds	Feedstock-S	3.5	55.4	6.2	1.4	37.0	2526	2919	7971	-
	SH	2.6	68.1	5.9	1.7	24.2	1456	3266	6177	96.5
	SAC	9.2	86.0	0.7	1.6	11.7	688	1679	3055	3.73
	SHAC	4.6	90.2	0.4	2.1	7.4	172	610	954	1.00
	SAK	3.3	84.8	0.7	0.3	14.2	451	2484	3386	2.24
	SHAK	2.1	90.5	0.5	0.2	8.7	569	2501	3640	2.03
Bagasse	Feedstock-B	6.0	50.9	5.9	1.3	41.9	3442	3731	10615	-
	BH	2.8	65.7	5.3	2.2	26.9	2719	8354	13792	67.6
	BAC	17.3	83.9	1.1	2.4	12.6	1437	3234	6109	6.24
	BHAC	6.5	89.7	0.9	2.5	6.9	303	1163	1769	1.95
	BAK	4.2	91.6	0.6	0.2	7.6	2063	4486	8612	6.45
	BHAK	0.1	88.8	0.4	0.4	10.3	1698	3621	7017	4.54
Stalks	Feedstock-R	6.0	47.2	5.8	0.8	46.1	3939	4230	12108	-
	RH	3.2	65.9	5.2	1.3	27.8	3380	5662	12422	126.8
	RAC	42.4	54.6	1.9	3.4	40.1	2730	8023	13483	64.5
	RHAC	5.2	86.3	2.2	1.8	9.8	2290	2776	7357	11.6
	RAK	2.1	88.7	0.4	0.2	10.7	2669	4568	9906	7.03
	RHAK	2.7	94.5	0.1	0.2	5.2	1138	3195	5471	3.58

Table 3.

Table 4.

Sample	N_2 adsorption					CO_2 adsorption		
	V_{pores}	$W_{o\text{-}N2}$	$L_{o\text{-}N2}$	S_{N2}	S_{BET}	$W_{o\text{-}CO2}$	$L_{o\text{-}CO2}$	S_{CO2}
SAC	0.22	0.22	0.63	703	535	0.23	0.53	819
SHAC	0.14	0.14	0.73	385	362	0.30	0.61	950
SAK	0.83	0.82	1.16	1511	2053	0.65	0.86	1512
SHAK	0.85	0.81	0.95	1791	2029	0.66	0.76	1768
BAC	0.34	0.32	0.82	803	809	0.31	0.60	979
BHAC	0.20	0.18	0.67	562	473	0.24	0.53	906
BAK	0.77	0.66	1.10	1301	1717	0.52	0.78	1335
BHAK	0.75	0.66	1.01	1367	1737	0.64	0.85	1545
RAC	-	0.09	1.22	164	230	0.07	0.67	209
RHAC	-	0.04	1.94	38	103	0.25	0.79	635
RAK	0.71	0.65	0.95	1408	1682	0.47	0.75	1295
RHAK	0.73	0.67	0.92	1529	1731	0.39	0.76	1051

Table 5.

Carbon	CO_2 uptake (wt.%)		Electrochemical capacitance	
	1 bar	20 bar	H_2SO_4	$EMImBF_4$/AN
SAC	9.9 (10.6)*	19.2	-	-
SHAC	11.8 (11.8)*	23.2	-	-
SAK	15.0	68.0	289	179
SHAK	15.8	68.9 (69.4)*	296	145
BAC	11.5	27.7	-	-
BHAC	9.8	15.9	-	-
BAK	13.9	55.1	262	142
BHAK	15.4	55.7	268	142
RAK	13.2	55.3 (58.3)*	269	160
RHAK	10.7	57.21	262	157

* (Experimental value)